

Diagnostic Accuracy of Non-melanocytic Pink Flat Skin Lesions on the Legs: Dermoscopic and Reflectance Confocal Microscopy Evaluation

Ignacio GÓMEZ-MARTÍN¹, Sara MORENO¹, Xavier DURAN², Ramon M. PUJOL¹ and Sonia SEGURA¹

¹Department of Dermatology, Hospital del Mar-Parc de Salut Mar, Departament de Medicina de la UAB, Universitat Autònoma de Barcelona,

²Department of Statistics, Institut Hospital del Mar d'Investigacions Mèdiques (IMIM), Barcelona, Spain

Pink flat skin lesions on the legs in elderly people represent a diagnostic challenge due to the paucity of clinical and dermoscopic evidence. A prospective study of 114 pink flat lesions on the legs of 85 elderly patients was performed to describe the utility of reflectance confocal microscopy in this clinical context. Evaluation of clinical, dermoscopic and confocal parameters and calculation of diagnostic accuracy/sensitivity/specificity for non-melanoma skin cancer diagnosis of each technique were carried out. Thirty-four benign and 80 malignant neoplasms were analysed. A correct clinical diagnosis was established in 49.1% of cases (sensitivity 68.7%, specificity 73.5%). Dermoscopy achieved 59.6% correct diagnosis (sensitivity 85%, specificity 67.6%) and confocal microscopy evaluation after clinical and dermoscopic evaluation rendered a correct diagnosis in 85.1% of cases (sensitivity 97.5%, specificity 88.2%). Confocal microscopy may improve diagnostic accuracy, sensitivity and specificity as a secondary evaluation after dermoscopy. A diagnostic confocal algorithm for pink flat lesions on the legs is proposed.

Key words: dermoscopy; reflectance confocal microscopy; histopathology; basal cell carcinoma; Bowen's disease; venous stasis dermatitis.

Accepted Aug 31, 2018; Epub ahead of print Sep 3, 2018

Acta Derm Venereol 2019; 99: 33–40.

Corr: Ignacio Gómez-Martín, Department of Dermatology, Hospital del Mar-Parc de Salut Mar. Universitat Autònoma de Barcelona, Passeig Marítim 25–29, ES-08003, Barcelona, Spain. E-mail: nachgm@gmail.com

Pink flat skin lesions on the legs of elderly people exhibit a broad differential diagnosis (1, 2). They represent a diagnostic challenge due to the paucity of clinical and dermoscopic morphological clues, and the existence of varying degrees of associated xerosis, sun damage and venous stasis dermatitis. Pink flat skin lesions often present with non-specific overlapping clinical and dermoscopic features (3–11).

Furthermore, on dermoscopy, pink lesions on the lower limbs usually exhibit prominent, but non-specific, vasculature due to orthostatic blood pressure.

Differential diagnosis includes tumoural lesions (Bowen's disease (BD), actinic keratosis (AK), invasive squamous cell carcinoma (SCC), basal cell carcinoma (BCC), amelanotic/hypomelanotic melanoma, seborr-

SIGNIFICANCE

Pink flat skin lesions on the legs represent a diagnostic challenge due to the paucity of specific clinical and dermoscopic features. A prospective study of a series of 114 pink flat skin lesions on the legs in elderly people was performed to describe the utility of reflectance confocal microscopy (RCM) in this clinical context. RCM resulted in 85.1% diagnostic accuracy, 97.5% sensitivity and 88.2% specificity for non-melanoma skin cancer diagnosis. A diagnostic RCM algorithm for pink flat lesions on the legs is proposed. RCM, as a secondary evaluation after dermoscopy, may improve diagnostic accuracy, sensitivity and specificity and may avoid the need for invasive biopsies.

hoic keratosis (SK), clear cell acanthoma, melanocytic naevus, angiomas, dermatofibroma, neurofibroma), inflammatory lesions (venous stasis dermatitis (VSD), lichen planus (LP), lichen planus-like keratosis (LPLK), porokeratosis, psoriasis, lichen aureus, lichen simplex chronicus) or infectious diseases (flat wart).

Dermoscopic algorithms used routinely for pigmented lesions are often not very helpful in the diagnosis of pink lesions. Several years ago, Giacomel & Zalaudek (12) suggested an algorithm for hypopigmented lesions based on vessel morphology, vascular architectural arrangement and additional criteria, and soon afterwards Zalaudek et al. (13) proposed including an initial clinical assessment and search for specific patterns. Rosendahl et al. (14) also described an algorithm for non-pigmented skin malignancies based on pattern analysis: first, looking for ulceration; secondly, for white clues; and thirdly, vessel analysis. However, these algorithms have not been tested in prospective studies for sensitivity, specificity or diagnostic accuracy.

In this particular clinical context, in which only scarce dermoscopic criteria are specific, reflectance confocal microscopy (RCM) may offer specific diagnostic criteria. RCM might achieve a confidence close to histopathology (gold standard) and may permit a decrease in the number of required biopsies, reducing costs and potential complications (pain, cellulitis and chronic ulcers).

The aim of the current study was to describe the utility of RCM in pink flat skin lesions on the legs in photodamaged skin, to characterize the dermoscopic and RCM criteria of the different skin conditions that present as

pink lesions on the legs, and to correlate the RCM findings with the corresponding histopathological features.

METHODS

Pink flat skin lesions on the legs in patients attending a referral unit in the Department of Dermatology, Hospital del Mar-Parc de Salut Mar were included prospectively between 1 January 2012 and 31 December 2016. The inclusion criteria used to recruit lesions to this study were: solitary pink flat lesions on the legs detected by clinical naked-eye examination with absent or less than 10% of pigmentation on dermoscopic evaluation. Only lesions for which skin cancer was suspected in the differential diagnosis were included in the study. Nodular lesions were excluded.

All patients gave written informed consent to be included in the study, which was approved by the ethics committee of our hospital.

Clinical and dermoscopic images of all lesions were obtained using a camera (PowerShot G10; Canon, Tokyo, Japan) attached to a contact polarized light dermoscopy device (DermLite Foto; 3Gen, San Juan Capistrano, CA, USA). No pressure was applied when taking image lesions, in order to preserve vessel morphology and ensure their better visualization. Dermoscopic images were evaluated blinded to histopathological diagnosis by one contributing author with >10 years of experience in the field (S.M.). A total of 49 dermoscopic criteria described in the literature were analysed during the evaluation.

RCM examination was performed in all lesions (VivaScope 1500; Caliber I.D., Rochester, NY, USA). Sequential images were recorded in horizontal 4×4 to 8×8 mm mosaics (VivaBlock; Caliber I.D.) at 3 levels of the skin (epidermis, dermal-epidermal junction and dermis) and vertical sequential images (VivaStack; Caliber I.D.) in the more representative areas of the lesion. RCM images were later evaluated by 2 authors (I.G.M, S.S.) with 5 and 12 years of experience, respectively, blinded to dermoscopic images and histopathological diagnosis. A total of 45 RCM criteria were investigated during the evaluation.

Dermoscopic and RCM criteria included in the evaluation process were selected based on the data available in the literature and in our preliminary observations. Each evaluator for both the dermoscopic and the confocal study was asked to assess the presence or absence of pre-defined dermoscopic and RCM structures and to provide a final diagnosis.

Diagnostic accuracy, sensitivity (number of malignant lesions correctly identified as such) and specificity (number of benign lesions correctly identified as such) were calculated after the independent assessment of clinical, dermoscopic and RCM images. In a second analysis such parameters were determined for RCM considering clinical, dermoscopic and RCM information in a real clinical setting.

One or more 4-mm punch biopsies were obtained from all lesions at the most suspicious areas after clinical, dermoscopic and RCM evaluation. Histopathological features were systematically evaluated by 3 dermatopathologists (IGM, RMP, SS). Thirty-six histopathological criteria were evaluated. Discrepant cases were consulted to an external pathologist. All histopathological evaluators were blinded to the clinical information and histopathological diagnosis.

In bivariate analysis dichotomous variables were evaluated by χ^2 test. In multivariate analysis of dermoscopic and RCM features a binary logistic regression was performed to differentiate between benign and malignant lesions. For the confocal, dermoscopic, and histopathological correlations, the Cohen kappa coefficient was calculated for each descriptor. Statistical evaluation was performed using SPSS statistical software for Windows, version 15.0 (SPSS Inc.).

RESULTS

A total of 114 pink flat skin lesions on the legs in 85 patients were included (57 women; 28 men), with a mean \pm standard deviation (SD) age of 73.18 ± 11.96 years. Ten lesions were located on the thighs and 104 on the lower legs. A total of 80 malignant lesions (50 BCC, 17 BD, 9 AK, 4 SCC) were analysed and 34 benign lesions (16 VSD, 5 SK, 3 psoriasis, 2 LPLK, 2 porokeratosis, 1 LP, 1 lichen simplex chronicus, 1 flat wart, 1 dermatofibroma, 1 neurofibroma, 1 hypertrophic scar).

Diagnostic accuracy/sensitivity/specificity (Table I)

Clinical evaluation. A correct clinical diagnosis was established in 49.1% of cases (56/114) and 70.2% (80/114) considering exclusively the diagnosis of benignity or malignancy. The sensitivity for malignant lesions was 68.7% (55/80) and the specificity for benign lesions was 73.5% (25/34).

Dermoscopy. Dermoscopy following clinical assessment achieved 59.6% (68/114) correct diagnosis and 79.8% (91/114) correct diagnoses when differentiating between benign or malignant. The sensitivity for malignant lesions was 85% (68/80) and the specificity for benign lesions was 67.6% (23/34).

Reflectance confocal microscopy. RCM evaluation blinded to clinical and dermoscopic images rendered a correct diagnosis in 71.9% of cases (82/114), and 85.1% (97/114) if only benignity or malignancy were considered. The sensitivity of RCM was 90% (72/80) and the specificity was 73.5% (25/34).

RCM evaluation after clinical and dermoscopic evaluation rendered a correct diagnosis in 85.1% of cases (97/114), and 94.7% (108/114) correct diagnoses when discriminating between benignity and malignancy. The sensitivity of RCM improved to 97.5% (78/80) and the specificity to 88.2% (30/34).

Dermoscopic features: bivariate and multivariate analysis

The most common criteria observed in BCC were the superficial scale, erosion/ulceration, white shiny structures, linear irregular vessels and clustered vessels (Table II). On the bivariate analysis multiple criteria, such as white shiny structures, erosion/ulceration, atypical vessels, ar-

Table I. Diagnostic accuracy, sensitivity and specificity of each technique

Technique	Diagnostic accuracy (benign/malignant) %	Diagnostic accuracy %	Sensitivity %	Specificity %
Clinical evaluation	70.2	49.1	68.7	73.5
Dermoscopy	79.8	59.6	85.0	67.6
bRCM	85.1	71.9	90.0	73.5
RCM	94.7	85.1	97.5	88.2

bRCM: reflectance confocal microscopy evaluation blinded to clinical and dermoscopic images; RCM: reflectance confocal microscopy evaluation.

Table II. Frequencies of dermoscopic and reflectance confocal microscopy parameters

	BCC group n = 50 n (%)	p-value ^a	BD/SCC group n = 30 n (%)	p-value ^b	Inflammatory disease group n = 25 n (%)	p-value ^c
<i>Dermoscopy</i>						
Erosion/ulceration	30 (60)	0.000 ^d	8 (26.7)	0.271	3 (12)	0.005 ^d
Scale	37 (74)	0.835	25 (83.3)	0.157	16 (64)	0.311
Cornoid lamella	0 (0)	0.255	0 (0)	0.565	3 (12)	0.01
Blue-grey ovoid nests	18 (36)	0.000	0 (0)	0.003	0 (0)	0.011
Multiple blue-grey globules	8 (16)	0.001	0 (0)	0.108	1 (4)	0.683
Spoke wheel-like structures/concentric (hub-like) structures	10 (20)	0.001	0 (0)	0.064	0 (0)	0.118
Maple leaf-like structures	5 (10)	0.014	0 (0)	0.323	0 (0)	0.584
Buck-shot scatter dots (in-focus blue/grey dots)	6 (12)	0.006	0 (0)	0.338	0 (0)	0.336
Pink-brownish eccentric structureless areas	6 (12)	0.097	12 (40)	0.002 ^d	1 (4)	0.041
Pink-white areas	15 (30)	0.063	6 (20)	1.000	2 (8)	0.096
White shiny structures (blotches and strands)	26 (52)	0.034 ^d	10 (33.3)	0.394	10 (40)	1.000
Atypical vessels	19 (38)	0.001	1 (3.3)	0.002	3 (12)	0.184
Arborizing vessels/ telangiectasia	17 (34)	0.001	2 (6.7)	0.057	1 (4)	0.041
Short fine telangiectasias	14 (28)	0.000 ^d	0 (0)	0.01	0 (0)	0.039
Glomerular vessels	18 (36)	0.038	21 (70)	0.005 ^d	14 (56)	0.370
Dotted vessels	19 (38)	0.023	19 (63.3)	0.138 ^d	16 (64)	0.176
Linear irregular vessels	24 (48)	0.000	5 (16.7)	0.102	2 (8)	0.006
Localized (clustered) vessels	24 (48)	1.000	19 (63.3)	0.055	8 (32)	0.112
Generalized vessels	17 (34)	0.440	8 (26.7)	0.132	16 (64)	0.005
Homogeneous vessels	6 (12)	0.000	13 (43.3)	0.174	16 (64)	0.000
Polymorphous vessels (≥2)	12 (24)	0.019	3 (10)	0.553	1 (4)	0.114
<i>Reflectance confocal microscopy</i>						
Parakeratosis	4 (8.2)	0.000	17 (58.6)	0.001	15 (60)	0.002
Hyperkeratosis	7 (14.3)	0.000	22 (75.9)	0.000 ^d	16 (64)	0.011
Ulceration/crust	25 (58.1)	0.071	17 (63)	0.071	5 (20.8)	0.005
Targetoid cells	1 (2)	0.001	11 (36.7)	0.000 ^d	3 (12)	1.000
Exocytosis	4 (8)	0.174	7 (23.3)	0.066	3 (12)	1.000
Spongiosis	0 (0)	0.066	2 (6.7)	0.606	3 (12)	0.069
Regular honeycomb	26 (53.1)	0.006	1 (3.3)	0.000	11 (44)	0.494
Streaming (polarized honeycomb)	32 (65.3)	0.000 ^d	4 (13.3)	0.003	4 (16)	0.032
Epidermal disarray	20 (40.8)	0.007	26 (86.7)	0.000 ^d	14 (56)	1.000
Non-visible papilla	40 (81.6)	0.000 ^d	16 (53.3)	0.279	11 (44)	0.06
Papillomatosis	1 (2)	0.137	0 (0)	0.187	5 (20)	0.006
Basal cords/nodules	32 (64)	0.000 ^d	1 (3.3)	0.000	1 (4)	0.001
Visible vessels	42 (85.7)	0.372	27 (100)	0.035	21 (91.3)	1.000
Telangiectasias	11 (22.4)	0.000	0 (0)	0.062	0 (0)	0.116
Round to S-shaped blood vessels	22 (44.9)	0.005	19 (70.4)	0.260	18 (78.3)	0.056
Convuluted glomerular vessels	24 (49)	1.000	13 (48.1)	1.000	15 (65.2)	0.102
Branched vessels	9 (18.4)	0.001	0 (0)	0.108	0 (0)	0.2
Curved linear vessels	19 (38.8)	0.008	8 (29.6)	0.619	1 (4.3)	0.007
Straight linear vessels	17 (34.7)	0.002	3 (11.1)	0.179	3 (13)	0.392
Polymorphic vessels (≥2)	28 (57.1)	0.000	9 (33.3)	0.819	2 (8.7)	0.001
Opposite flows	8 (16.3)	0.064	2 (7.4)	0.727	1 (4.3)	0.451
Melanophages	31 (64.6)	0.000	9 (32.1)	0.128	7 (30.4)	0.156
Dermal inflammatory cells	1 (2.1)	0.216	1 (3.6)	1.000	4 (17.4)	0.02 ^d
Thickened collagen bundles	34 (82.9)	0.000	2 (11.8)	0.001	2 (15.4)	0.012

^aBCC vs non-BCC. ^bBD/SCC vs non-BD/SCC. ^cInflammatory vs non-inflammatory. ^dSignificant criteria on multivariate analysis.
BCC group: basal cell carcinoma group. BD/SCC group: group including Bowen's disease, actinic keratosis and squamous cell carcinoma.

borizing vessels/telangiectasia, short fine telangiectasia, linear irregular vessels, polymorphous vessels, multiple blue-grey globules, leaf-like structures, blue-grey ovoid nests, buck-shot scatter dots (in-focus dots) and spoke wheel-like structures/concentric structures were statistically significant.

On the multivariate analysis white shiny structures ($p=0.027$), erosion/ulceration ($p=0.000$) and short fine telangiectasias ($p=0.005$) were statistically significant.

The most common dermoscopic features in the BD/SCC group were the superficial scale, glomerular vessels, dotted vessels and localized vessels (Table II). Dermoscopy of BD/SCC group exhibited 2 statistically significant criteria that were glomerular vessels and pink-

brownish eccentric structureless areas. On the multivariate analysis pink-brownish eccentric structureless areas ($p=0.001$), dotted vessels ($p=0.021$) and glomerular vessels ($p=0.017$) were statistically significant.

The most common dermoscopic features of the inflammatory group were the superficial scale, white shiny structures, glomerular, dotted, homogeneous and generalized vessels (Table II). Three criteria were statistically significant on the bivariate analysis: homogeneous vessels, generalized vessels and cornoid lamella. On the multivariate analysis only erosion/ulcer was a statistically significant protector criteria ($p=0.031$).

The most frequent dermoscopic criteria in VSD were superficial scale (68.75%, 11/16), glomerular ves-

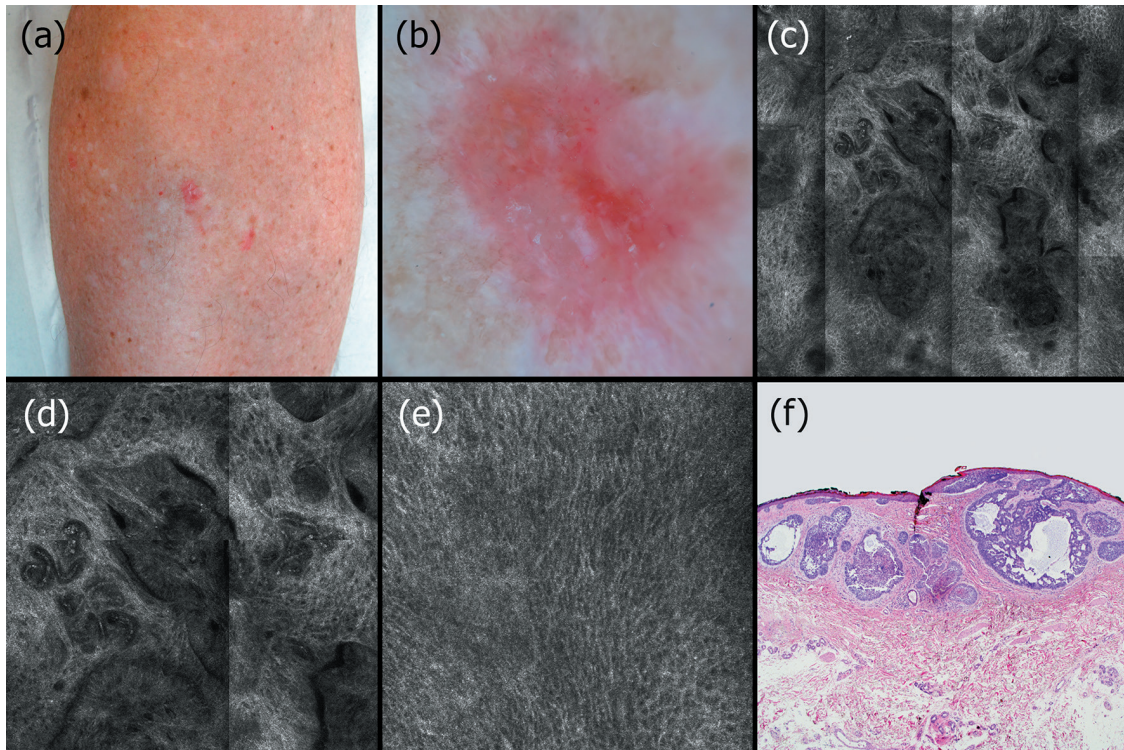


Fig. 1. Basal cell carcinoma. (a) Pink plaque on the right leg in a man in his 60s. (b) Dermoscopic image showed a superficial scale, pink-white areas, white shiny structures, generalized, atypical, polymorphous vessels (linear irregular vessels, short fine arborizing vessels, glomerular vessels). (c) Reflectance confocal microscopy (RCM) mosaic (1.5×1.5 mm) at the dermal-epidermal junction (DEJ) showing multiple clefted basaloid nodules, polymorphic vessels and thickened collagen bundles. (d) RCM image (0.5×0.5 mm). Detail of basaloid nodules and polymorphic vessels (branching vessels and convoluted glomerular vessels). (e) RCM image (0.5×0.5 mm). Polarized honeycomb on suprabasal layers. (f) Biopsy specimen revealed a nodular basal cell carcinoma. Haematoxylin-eosin, original magnification ×100.

sels (62.5%, 10/16), dotted and homogeneous vessels (56.25%, 9/16), generalized vessels (50%, 8/16) and white shiny structures (50%, 8/16). Generalized vessels ($p=0.026$) and homogeneous vessels ($p=0.002$) were statistically significant in multivariate analysis.

Reflectance confocal microscopy features: bivariate and multivariate analysis

RCM criteria more frequently observed in BCC (**Fig. 1**) were ulceration/crust, streaming, non-visible papilla, basal cords/nodules, visible vessels, polymorphic vessels, convoluted glomerular vessels, melanophages and thickened collagen bundles (Table II). On bivariate analysis regular honeycomb, streaming (polarized honeycomb), non-visible papilla, basal cords/nodules, telangiectasias, branched vessels, curved vessels, straight vessels, polymorphic vessels, thickened collagen bundles and melanophages were statistically significant. Basal cords/nodules ($p=0.000$), streaming ($p=0.001$) and non-visible papilla ($p=0.03$) reached statistical significance on multivariate analysis.

Hyperkeratosis, parakeratosis, ulceration/crust, epidermal disarray, visible vessels and round to S-shaped blood vessels were the criteria most often observed in BD/SCC group (Table II, **Fig. 2**). Statistically significant RCM criteria on the bivariate analysis in BD/SCC group were

parakeratosis, hyperkeratosis, targetoid cells, epidermal disarray and visible vessels. On multivariate analysis hyperkeratosis ($p=0.005$), targetoid cells ($p=0.044$) and epidermal disarray ($p=0.012$) were statistically significant.

In the inflammatory group, the RCM criteria most frequently observed were hyperkeratosis, parakeratosis, visible vessels, round to S-shaped and convoluted glomerular vessels (Table II). RCM criteria on the inflammatory group that were statistically significant on the bivariate analysis were parakeratosis, hyperkeratosis, non-edged papilla, papillomatosis and dermal inflammatory cells. On multivariate analysis the presence of dermal inflammatory cells ($p=0.034$) was statistically significant.

The most common criteria in VSD were visible vessels, round to S-shaped and convoluted glomerular vessels (**Fig. 3**). Statistically significant RCM criteria of VSD on bivariate analysis were parakeratosis ($p=0.045$), spongiosis ($p=0.019$), convoluted glomerular vessels ($p=0.012$), dermal inflammatory cells ($p=0.037$) and huddles of collagen ($p=0.048$). No criterion was statistically significant on multivariate analysis.

Correlation between techniques

Dermoscopy – reflectance confocal microscopy. Classical criteria of pigmented BCC (blue-grey ovoid nests, leaf-like structures, spoke wheel/concentric structures

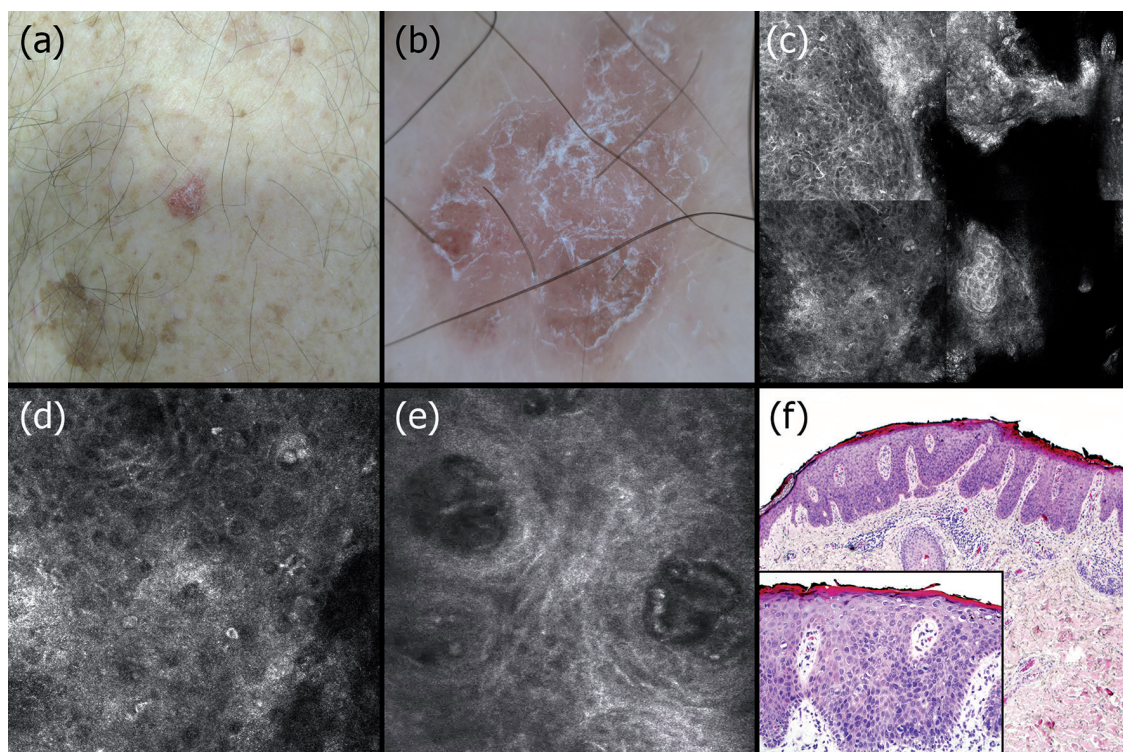


Fig. 2. Bowen's disease. (a) Pink plaque on the left thigh of a man in his 70s. (b) Dermoscopic image revealed superficial scale, pink-brownish eccentric structureless area and localized, homogeneous, dotted and glomerular vessels. (c) RCM mosaic (1×1 mm) at suprabasal layers exhibiting epidermal disarray and parakeratosis. (d) RCM image (0.5×0.5 mm). Detail of an atypical honeycomb pattern with targetoid cells and multinucleated cells in granular/spinous layer of epidermis. (e) RCM image (0.5×0.5 mm) at superficial papillary dermis showing round to S-shaped and convoluted glomerular vessels. (f) Biopsy specimen revealed hyperkeratosis, parakeratosis, acanthosis and full-thickness dysplasia of epidermis. Haematoxylin-eosin (H&E), original magnification ×100. *Inset*: detail of epidermal dysplasia with keratinocyte atypia, atypical mitosis, multinucleated cells and dyskeratotic cells (H&E, original magnification ×200).

and buck-shot scatter dots) correlated with moderate agreement with basal cords/nodules on RCM ($k=0.426$, $p=0.000$). Short fine telangiectasias correlated well with branched vessels on RCM ($k=0.442$, $p=0.000$), whereas ulceration/erosion on dermoscopy correlated with ulceration/crust on RCM ($k=0.470$, $p<0.001$).

Reflectance confocal microscopy – histopathology. Among the RCM criteria, basaloid cords/nodules correlated well with basaloid nests on histopathology ($k=0.631$, $p=0.000$) and clefting on RCM with clefting on histopathology ($k=0.607$, $p=0.000$). Targetoid cells seen in BD by RCM had a good correlation with atypical mitosis on histopathology ($k=0.455$, $p=0.045$). Thickened collagen bundles on RCM correlated well with desmoplasia on histopathology with moderate agreement ($k=0.439$, $p=0.000$).

Some RCM criteria had poor correlation with their counterparts on histopathological examination: parakeratosis ($k=0.335$, $p=0.000$), hyperkeratosis ($k=0.362$, $p=0.000$), epidermal atypia (epidermal disarray on RCM) ($k=0.380$, $p=0.000$), or intratumoral melanin in basal cords/nodules ($k=0.359$, $p=0.001$).

Dermal structures, such as inflammation, vascularization and melanophages, presented very poor correlation between RCM and histopathology.

DISCUSSION

Pink flat lesions on the legs of elderly people are frequently seen in dermatologist consultations. Such lesions comprise a heterogeneous group of entities with different clinical significance and management, varying from inflammatory conditions to skin cancer. Clinical and dermoscopic diagnosis may be difficult due to lack of specific criteria. In order to establish a definite diagnosis, biopsies are frequently required, which is a procedure that in this clinical setting is not devoid of potential complications (ulceration or infection).

In recent years, multiple authors have described dermoscopic patterns of hypopigmented lesions, mainly based on vascularization (1–14).

We have observed, in agreement with patterns described in the literature, that BD is typically characterized by superficial scales and glomerular/dotted vessels arranged in clusters, superficial BCC by short fine telangiectasias, shiny pink-white areas and multiple small erosions, and VSD is defined by a scaly surface and homogeneous glomerular/dotted vessels in a generalized distribution.

However, important dermoscopic criteria (especially vascular criteria, such as glomerular/dotted vessels or scaly surface) overlap among different entities represen-

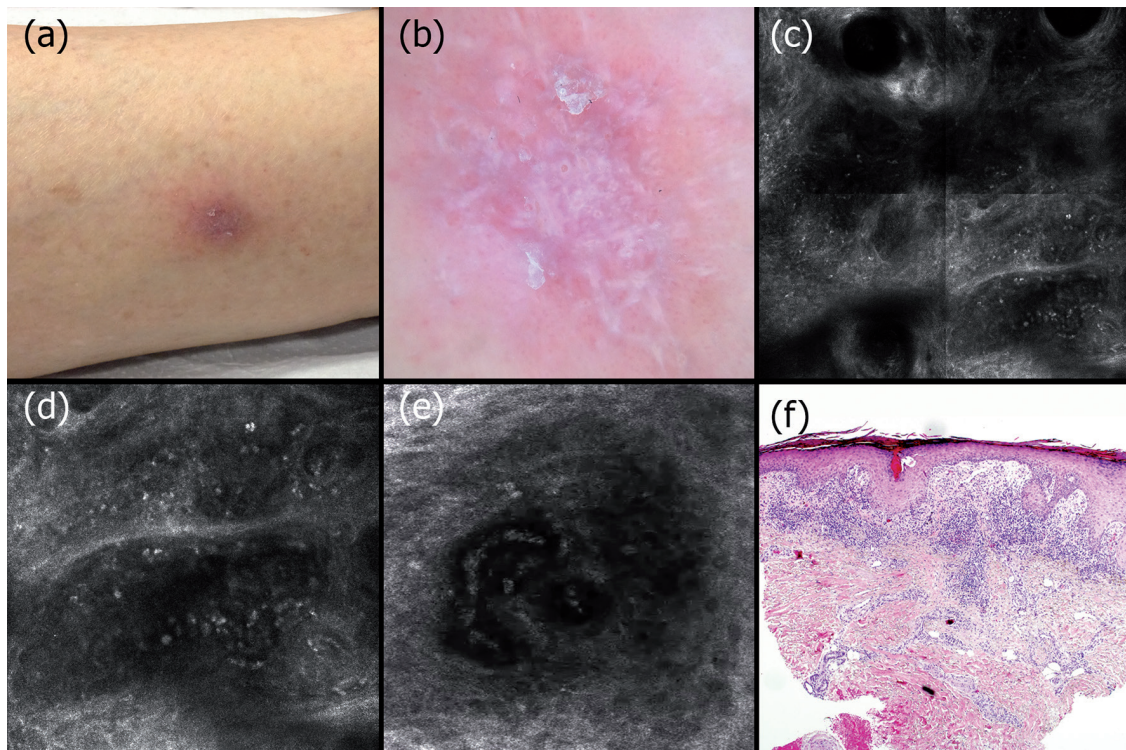


Fig. 3. Venous stasis dermatitis. (a) Pink plaque on the right leg of a woman in her 70s. (b) Dermoscopic image exhibited superficial scales, white shiny structures, multiple rosette signs, white circles and generalized and homogeneous dotted vessels. (c) Reflectance confocal microscopy (RCM) mosaic (1×1 mm) at the dermal-epidermal junction revealing exocytosis, dermal inflammatory cells and melanophages. (d) RCM image (0.5×0.5 mm). Detail of the inflammatory cells and exocytosis. (e) RCM image (0.5×0.5mm). Round to S-shaped blood vessels in the centre of dermal papilla. (f) Biopsy specimen revealed hyperkeratosis, parakeratosis and acanthosis of the epidermis, and a dense, predominantly lymphocytic inflammatory infiltrate and dilated capillaries on the papillary dermis. Haematoxylin-eosin, original magnification ×100.

ting a decrease in dermoscopic specificity and diagnostic accuracy in the lower limbs.

RCM is a non-invasive real-time technique that has been useful in the diagnosis of skin cancer and inflammatory skin diseases. Recently, multiple hypopigmented lesions have been described by means of RCM (15–28) trying to help clinicians to decide confidently whether a pink lesion should be biopsied. Thus, techniques such as RCM may avoid unnecessary biopsies and allow monitoring of the response to non-invasive treatments, such as photodynamic therapy, topical imiquimod, ingenol mebutate gel, topical diclofenac or topical 5-fluorouracil (29–34).

In a prospective blinded design we observed that clinical and dermoscopic evaluation have an elevated rate of misdiagnosis in pink flat lesions on the legs, whereas RCM improves diagnostic accuracy. In clinical evaluation, we observed a tendency to underestimate malignant pink lesions; whereas in dermoscopic evaluation, due to high presence of vascularity in pink lesions on the legs, we tended to overestimate malignancy. Dermoscopy presented low diagnostic accuracy (59.6%), moderately good sensitivity (85%), but low specificity (67.6%), even lower than clinical examination. In our study, blinded RCM has demonstrated higher levels of sensitivity (90%), specificity (73.5%) and diagnostic ac-

curacy (71.9%). In a more realistic model, in which RCM assessment was performed after clinical and dermoscopic evaluation, diagnostic values increased to 97.5%, 88.2% and 85.1%, respectively. These results highlight dermoscopy and RCM as complementary/synergistic techniques for diagnosing pink flat lesions on the legs.

In concordance with the literature, our study showed through multivariate analysis the following significant RCM criteria in BCC: basal cords/nodules, streaming and non-visible papilla (15, 16). Basal cords/nodules had a good correlation with classical dermoscopic criteria of pigmented BCC and with the presence of basaloid nests in histopathology. The BD/SCC group showed, as previously reported: hyperkeratosis, targetoid cells and epidermal disarray (17, 21, 23, 24). Interestingly, targetoid cells had a good correlation with atypical mitosis. Finally, the inflammatory group showed the presence of dermal inflammatory cells, as in previous reports (26). However, the agreement with histopathological inflammation was poor, probably because it is difficult to assess dermal features by RCM.

Other criteria, such as spongiosis, parakeratosis and round to S-shaped blood vessels, did not show significant association with the inflammatory group due to the small number of cases and the presence of these criteria in some cases in the BD/SCC group.

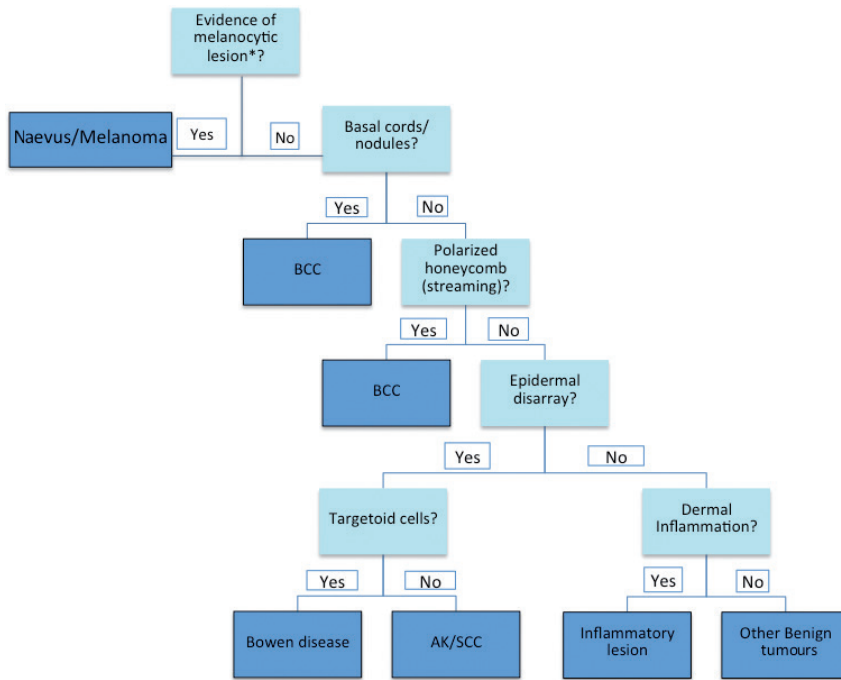


Fig. 4. Reflectance confocal microscopy (RCM) algorithm. *Junctional nests/thickenings, dermal nests, widespread atypical cells at dermal-epidermal junction. BCC: basal cell carcinoma; AK: actinic keratosis; SCC: squamous cell carcinoma.

Surprisingly, multivariate analysis did not show significance of any kind of vessels; perhaps due to a higher prevalence of vascularity in the lower limbs, frequent overlapping of vascular patterns among different entities, and technical difficulties when evaluating dermal features in hyperkeratotic lesions.

In view of these results, we propose a RCM algorithm (Fig. 4) to improve the diagnosis of pink flat skin lesions on the legs, in which the main criteria are obtained from the results of multivariate analysis. An initial step has been added to this algorithm to rule out a melanocytic lesion, in accordance with other RCM algorithms (18) proposed in solitary pink lesions, since the screening of malignant melanoma is essential when evaluating a cutaneous pink lesion.

Study limitations

No case of amelanotic/hypomelanotic melanoma could be included in our series because of the low prevalence (2–8%) of this subtype of malignant melanoma (10).

Definite diagnosis was established according to a 4-mm punch evaluation chosen by RCM findings in all cases, which may have caused confocal false negatives according to histopathology if the sample was not perfectly representative of the lesion.

Thick hyperkeratosis, ulceration and crusts represented a technical limitation in the dermoscopic-RCM-histopathology correlation, because they may have hampered the quality of RCM imaging or not allowed sufficient penetration of RCM light to reliably assess dermal features.

Larger series with different pink tumours (especially melanoma) and inflammatory/infectious conditions should be studied to confirm our results.

Conclusion

This study demonstrated that, in this clinical setting, where clinical evaluation and dermoscopy do not possess high specificity, RCM might be a useful tool, since, importantly, it may improve diagnostic accuracy, sensitivity and specificity for non-melanoma skin cancer diagnosis, thus reducing the number of biopsies and their consequences (pain, costs, scars, infections and chronic ulcers).

ACKNOWLEDGEMENTS

Additional contributions: Carlos Barranco, MD (Department of Pathology, Hospital del Mar-Parc de Salut Mar, Universitat Autònoma de Barcelona, Spain) helped with histopathological examination in discrepant cases. There was no financial compensation other than salary.

Additional information: This work was conducted within the framework of the PhD in medicine for Dr Gómez-Martin from the Universitat Autònoma de Barcelona. Biological samples were obtained from Parc de Salut MAR Biobank, Barcelona.

Funding source: This work was supported by grants RD09/0076/00036 and PT13/0010/0005 from Instituto de Salud Carlos III/FEDER and the Xarxa de Bancs de tumors, sponsored by Pla Director d'Oncologia de Catalunya.

The authors have no conflicts of interest to declare.

REFERENCES

- Zalaudek I, Kreusch J, Giacomel J, Ferrara G, Catricalà C, Argenziano G. How to diagnose nonpigmented skin tumors: a review of vascular structures seen with dermoscopy: part II. Nonmelanocytic skin tumors. *J Am Acad Dermatol* 2010; 63: 377–386.
- Zalaudek I, Kreusch J, Giacomel J, Ferrara G, Catricalà C, Argenziano G. How to diagnose nonpigmented skin tumors: a review of vascular structures seen with dermoscopy: part

- I. Melanocytic skin tumors. *J Am Acad Dermatol* 2010; 63: 361–374.
3. Zalaudek I. Dermoscopy subpatterns of nonpigmented skin tumors. *Arch Dermatol* 2005; 141: 532.
 4. Martín JM, Bella-Navarro R, Jordá E. Vascular patterns in dermoscopy. *Actas Dermosifiliogr* 2012; 103: 357–375.
 5. Altamura D, Menzies SW, Argenziano G, Zalaudek I, Soyer HP, Sera F, et al. Dermatoscopy of basal cell carcinoma: morphologic variability of global and local features and accuracy of diagnosis. *J Am Acad Dermatol* 2010; 62: 67–75.
 6. Micantonio T, Gulia A, Altobelli E, Di Cesare A, Fidanza R, Riitano A, et al. Vascular patterns in basal cell carcinoma. *J Eur Acad Dermatol Venereol* 2011; 25: 358–361.
 7. Zaballos P, Salsench E, Puig S, Malvey J. Dermoscopy of venous stasis dermatitis. *Arch Dermatol* 2006; 142: 1526.
 8. Zaballos P, Puig S, Malvey J. Dermoscopy of pigmented purpuric dermatoses (lichen aureus): a useful tool for clinical diagnosis. *Arch Dermatol* 2004; 140: 1290–1291.
 9. Zalaudek I, Argenziano G, Leinweber B, Citarella L, Hofmann-Wellenhof R, Malvey J, et al. Dermoscopy of Bowen's disease. *Br J Dermatol* 2004; 150: 1112–1116.
 10. Pizzichetta MA, Talamini R, Stanganelli I, Puddu P, Bono R, Argenziano G, et al. Amelanotic/hypomelanotic melanoma: clinical and dermoscopic features. *Br J Dermatol* 2004; 150: 1117–1124.
 11. Pan Y, Chamberlain AJ, Bailey M, Chong AH, Haskett M, Kelly JW. Dermatoscopy aids in the diagnosis of the solitary red scaly patch or plaque-features distinguishing superficial basal cell carcinoma, intraepidermal carcinoma, and psoriasis. *J Am Acad Dermatol* 2008; 59: 268–274.
 12. Giacomel J, Zalaudek I. Pink lesions. *Dermatol Clin* 2013; 31: 649–678.
 13. Zalaudek I, Argenziano G, Giacomel J. Dermatoscopy of non-pigmented skin tumors: Pink-Think-Blink. Boca Raton, FL: CRC Press; 2015.
 14. Rosendahl C, Cameron A, Tschandl P, Bulinska A, Zalaudek I, Kittler H. Prediction without pigment: a decision algorithm for non-pigmented skin malignancy. *Dermatol Pract Concept* 2014; 4: 59–66.
 15. Gonzalez S, Tannous Z. Real-time, in vivo confocal reflectance microscopy of basal cell carcinoma. *J Am Acad Dermatol* 2002; 47: 869–874.
 16. Guitera P, Menzies SW, Longo C, Cesinaro AM, Scolyer RA, Pellacani G. In vivo confocal microscopy for diagnosis of melanoma and basal cell carcinoma using a two-step method: analysis of 710 consecutive clinically equivocal cases. *J Invest Dermatol* 2012; 132: 2386–2394.
 17. Peppelman M, Nguyen KP, Hoogedoorn L, van Erp PE, Gerritsen MJ. Reflectance confocal microscopy: non-invasive distinction between actinic keratosis and squamous cell carcinoma. *J Eur Acad Dermatol Venereol* 2015; 29: 1302–1309.
 18. Gill M, González S. Enlightening the pink: use of confocal microscopy in pink lesions. *Dermatol Clin* 2016; 34: 443–458.
 19. Braga JC, Scope A, Klaz I, Mecca P, González S, Rabinovitz H, Marghoob AA. The significance of reflectance confocal microscopy in the assessment of solitary pink skin lesions. *J Am Acad Dermatol* 2009; 61: 230–241.
 20. Longo C, Moscarella E, Argenziano G, Lallas A, Raucci M, Pellacani G, Scope A. Reflectance confocal microscopy in the diagnosis of solitary pink skin tumours: review of diagnostic clues. *Br J Dermatol* 2015; 173: 31–41.
 21. Ulrich M, Maltusch A, Rius-Diaz F, Röwert-Huber J, González S, Sterry W, Stockfleth E, Astner S. Clinical applicability of in vivo reflectance confocal microscopy for the diagnosis of actinic keratoses. *Dermatol Surg* 2008; 34: 610–619.
 22. Nori S, Rius-Diaz F, Cuevas J, Goldgeier M, Jaen P, Torres A, González S. Sensitivity and specificity of reflectance-mode confocal microscopy for in vivo diagnosis of basal cell carcinoma: a multicenter study. *J Am Acad Dermatol* 2004; 51: 923–930.
 23. Ulrich M, Kanitakis J, González S, Lange-Asschenfeldt S, Stockfleth E, Roewert-Huber J. Evaluation of Bowen disease by in vivo reflectance confocal microscopy. *Br J Dermatol* 2012; 166: 451–453.
 24. Rishpon A, Kim N, Scope A, Porges L, Oliviero MC, Braun RP, et al. Reflectance confocal microscopy criteria for squamous cell carcinomas and actinic keratoses. *Arch Dermatol* 2009; 145: 766–772.
 25. Ardigò M, Soyer HP. Reflectance confocal microscopy for better management of cutaneous pink lesions. *Br J Dermatol* 2015; 173: 6–7.
 26. Ardigo M, Longo C, Gonzalez S. Multicentre study on inflammatory skin diseases from The International Confocal Working Group: specific confocal microscopy features and an algorithmic method of diagnosis. *Br J Dermatol* 2016; 175: 364–374.
 27. Incel P, Gurel MS, Erdemir AV. Vascular patterns of nonpigmented tumoral skin lesions: confocal perspectives. *Skin Res Technol* 2015; 21: 333–339.
 28. Losi A, Longo C, Cesinaro AM, Benati E, Witkowski A, Guitera P, Pellacani G. Hyporeflexive pagetoid cells: a new clue for amelanotic melanoma diagnosis by reflectance confocal microscopy. *Br J Dermatol* 2014; 171: 48–54.
 29. Ulrich M, Lange-Asschenfeldt S, Gonzalez S. The use of reflectance confocal microscopy for monitoring response to therapy of skin malignancies. *Dermatol Pract Concept* 2012; 2: 202a10.
 30. Longo C, Casari A, Pepe P, Moscarella E, Zalaudek I, Argenziano G, Pellacani G. Confocal microscopy insights into the treatment and cellular immune response of Basal cell carcinoma to photodynamic therapy. *Dermatology* 2012; 225: 264–270.
 31. Seyed Jafari SM, Timchik T, Hunger RE. In vivo confocal microscopy efficacy assessment of daylight photodynamic therapy in actinic keratosis patients. *Br J Dermatol* 2016; 175: 375–381.
 32. Longo C, Borsari S, Benati E, Moscarella E, Alfano R, Argenziano G. Dermoscopy and reflectance confocal microscopy for monitoring the treatment of actinic keratosis with ingenol mebutate gel: report of two cases. *Dermatol Ther (Heidelb)* 2016; 6: 81–87.
 33. Ulrich M, Lange-Asschenfeldt S, Skak K, Skov T, Østerdal ML, Röwert-Huber HJ, et al. Biological effects of ingenol mebutate gel in moderate to severe actinic fields assessed by reflectance confocal microscopy: a phase I study. *J Drugs Dermatol* 2016; 15: 1181–1189.
 34. Malvey J, Roldán-Marín R, Iglesias-García P, Díaz A, Puig S. Monitoring treatment of field cancerisation with 3% diclofenac sodium 2.5% hyaluronic acid by reflectance confocal microscopy: a histologic correlation. *Acta Derm Venereol* 2015; 95: 45–50.